

Using Taguchi Technique to Study the Effect of Adding Copper Nano on Shape Recovery for Smart Alloy (CU-AL-NI)

Dilsuz A. Abdaljabar  *, Ahmed Abdulrasool Ahmed AL-Khafaji  

Department of Mechanical Engineering, College of Engineering, University of Baghdad, Baghdad, Iraq

ABSTRACT

This research aims to reduce the number of experiments by using the Taguchi technique. It will be applied on adding copper nano particles and study its effect on shape recovery for a shape memory alloy (83% Cu- 13% Al- 4%Ni). Different proportions of nano were added to the alloy in return for changing the proportion of copper while maintaining the proportions of nickel and aluminum constant. Powder metallurgy technique was used to manufacture the samples. Two types of tests were performed: physical tests, including X-ray diffraction (XRD) and scanning electron microscopy (SEM), were used to inspect raw materials before manufacturing and to inspect samples after manufacturing. A mechanical test of the shape memory effect (SME%) was conducted for different a compression ratio. The results indicate that the addition of copper nano particles reduces shape recovery at a compression ratio of 3%. Analysis of results represented by Signal to Noise ratio (S/N) and ANOVA show the most significant factor in shape recovery was copper nano particles followed by copper particles and the most contribution factor was copper nano particles in percentage 87.82%.

Keywords: Analysis of variance, Cu nano, Shape memory alloy, Shape memory effect, Powder metallurgy, Taguchi method.

1. INTRODUCTION

Shape memory alloys (SMAs) are intelligent materials that can undergo the martensitic phase transformation when thermo mechanical loads are applied and they can also return to their original form when heated above certain temperatures (**Otsuka and Wayman, 1999**). SMAs exist in two crystal phases: the parent phase austenite is stable at high temperatures, and the product phase, known as martensite, is stable at low temperatures (**Christian, 2013**). When the SMA was in the martensite phase, it readily deformed due to its relative softness (**Mohammed and Shahatha, 2023**). The most important properties of

*Corresponding author

Peer review under the responsibility of University of Baghdad.

<https://doi.org/10.31026/j.eng.2025.05.03>

© 2025 The Author(s). Published by the College of Engineering, University of Baghdad



This is an open access article under the CC BY 4 license (<http://creativecommons.org/licenses/by/4.0/>).

Article received: 19/10/2024

Article revised: 12/01/2025

Article accepted: 21/02/2025

Article published: 01/05/2025

shape-memory alloys are pseudo-elasticity and shape-memory effect (SME) characteristics, which have allowed shape-memory alloys to stand out from other kinds of materials (Malinin et al., 2018). Thermoelastic martensitic transformation is made possible by the shape memory effect (SME) of SMAs. The deformation of the SMA during loading and unloading at temperatures lower than the Martensite finish will result in the shape memory effect during the martensitic phase (Morales et al., 2018). These distorted alloys regain their original shape when heated to a temperature higher than the Austenite finish, which forms the austenite phase, as shown in Fig. 1 (Najah, 2020).

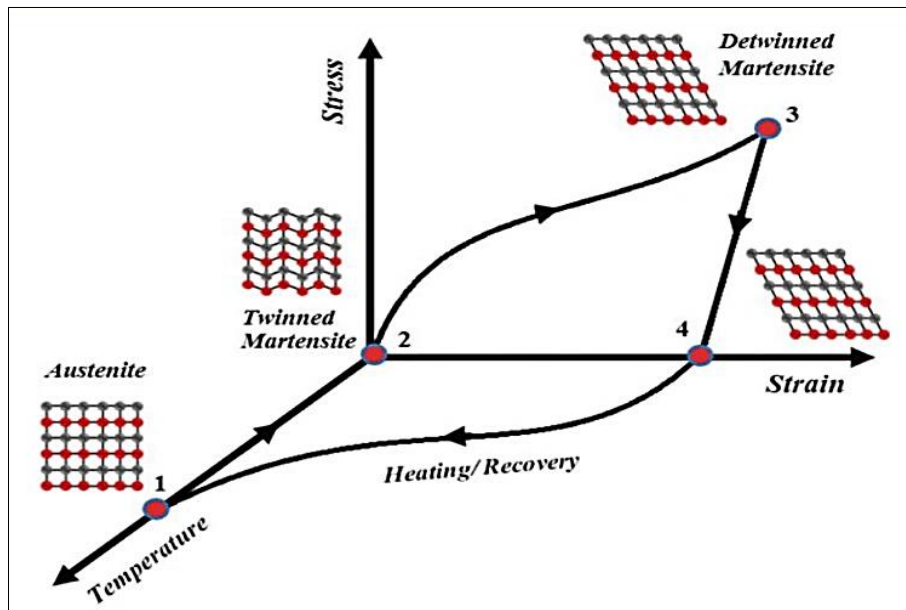


Figure 1. Schematic diagram of stress-strain-temperature for the involved crystallographic changes during the phenomena of SME (Lagoudas, 2008).

The cooling process causes the parent phase to change into the twinned martensite (1 → 2). When the materials are loaded, inelastic strains and stress-induced detwinning may happen (2 → 3). Even after the unloaded process, the martensite phase remains in the same state as the de-twinned structure with no recovered inelastic strains (3 → 4). Ultimately, the materials are heated above the Austenite finish (4 → 1) to recover the inelastic strains and return to their original shape (Othmane, 2020; Corneliu, 2010). Since Shape Memory Alloy has so many uses and excellent qualities, it is used extensively in many engineering fields, like SMA in fuel injectors, thermal valves, SMA gloves, and SMA isolation devices for elevated highway bridges (Sadashiva et al., 2021; Manianb, 2021). And also in medical applications, like implants, prostheses, and rehabilitation devices (Gabriele et al., 2023). The Taguchi experiment array design is a statistical tool developed by Japanese engineer Genier Taguchi that provides a model for designing experiments. It arranges process parameters and the levels at which they should be varied. Taguchi's design reduces costs, time, and resource requirements (Amir and Anuradha, 2018). Taguchi's optimization method is the most effective tool for designing different types of manufacturing systems. The right orthogonal array is developed for the optimal process parameters, where the variance should be low, based on carefully planned experiments. Integration is achieved for the Taguchi method using a suitable design of experiments (DOE) to streamline the process



(Kumar L, 2017). The DoE Taguchi method's characteristics, as previously stated, lower the number of experiments and, consequently, the overall experiment cost **(Safi et al., 2024)**. The required data can be obtained through an experimental plan that is provided by the Taguchi technique. Two available methods for analyzing the data are the analysis of variance (ANOVA) **(Nashwan et al., 2024)**. And the signal-to-noise (S/N) ratio **(Omkar, 2021)**. There are many studies on the impact of the addition of nanoparticles on the physical and mechanical properties of smart alloy (Cu- Al- Ni) SMEs as well as studies on the use of the Taguchi technique to optimized process parameter.

(Safaa et al., 2014) studied the effect of adding silver nanoparticles to (Cu-Al-Ni) SMAs on phase transformation and mechanical properties. The microstructural changes and mechanical properties were investigated using field emission scanning electron microscopy, X-ray diffraction tensile test and shape memory effect test. It was found that the addition of Ag can control the phase morphology and orientations and shape memory effect is improved. The shape recovery ratio reached approximately 80% of the original shape.

(Sara, 2015) got the best mechanical properties with the fewest tests possible, the Taguchi method was applied. An orthogonal array OA (L9) with three distinct levels and two distinct parameters (temperature and pressure). Powder metallurgy was to manufacture the (CU-AL-NI) alloy samples. There were two different kinds of tests run: mechanical and physical. The goal of the physical examinations is to identify the alloy's phases. To determine the best combination of effective parameters, the mechanical properties testing results were incorporated into the Taguchi method. The shape memory effect was best affected by the sintering temperature, according to the results.

(Ahmed and Sara, 2016) In this work, powder metallurgy was used to create the samples for the smart alloy, which is made up of Copper alloy, Aluminum, and Nickel. The powder was compacted at three different pressure values (300, 500, and 700 MPa) and three different sintering temperature values (700, 800, and 900 °C). Carried out the required testing, including a resilience screening on each sample. According to the experimental test on the samples, the resilient value peaked at 700 MPa of pressure and 900 °C of sintering temperature.

(Hasan and Ahmed, 2018) A Cu-Al-Ni alloy was created using the powder metallurgy method, which involved mixing 83%Cu-13%Al-4%Ni powder for six hours. Then (3,4,5,6,7) hours of sintered at 850 °C and compacted at 650 Mpa. Samples were subjected to mechanical testing (recovery test) and physical testing (XRD, SEM). The shape recovery increased with the amount of sintering time, as demonstrated by the results.

(Ahmed, 2018) The effects of two alloy elements, Cu and AL, on the mechanical and physical characteristics of Cu-Al-Ni were studied The standard weight percentage of this alloy is [83%Cu-13%Al-4%Ni]. Using the powder metallurgy technique, four distinct weight percentages of elements (Cu-Al) were selected. The maximum value of shape recovery, according to the sample test results, is (83%), which appeared in the weight percentage [82%Cu-14%Al-4%Ni]. In contrast, no shape recovery was seen in the samples in the weight percentages [78% Cu-18%Al-4%Ni], [80% Cu-16%Al-4%Ni], due to increasing brittleness and decreasing toughness with an increase in Al% content, which caused failure in these proportions.

(Raed et al., 2018) The Effects of incorporating carbon nanotubes (CNTs) into shape memory alloy (SMA) were investigated. The percentages of carbon nanotube addition were (0, 0.5, 1, 2, and 2.5) % about the copper ratio (83% Cu, 13% Al, 4% Ni). Powder metallurgy (PM) was used in the manufacturing of the samples. The findings demonstrated that raising



the concentration of carbon nanotubes (CNTs) to 2.5% increased the hardness by the same amount of CNTs. The hardness decreases with increasing concentrations (0, 0.5, 1, 2) %.

(Raed and Omer, 2020) The effect of adding Mg particles on mechanical properties. The Mg particles were added in a percentage (0.25, 0.5, 0.75, 1, and 1.25%) to a smart alloy (Cu 83%-Al 13%-Ni 4%) as the volumetric percentage was taken from Copper percentage. The samples were manufactured by (PM) Technique. The mechanical shows the enhancement in properties, hardness increases when increase Mg percentage and an increase in transformation temperature with an increase in Mg percentage.

(Samudrapom, 2022) The effect of adding Al₂O₃ Nano particles on the mechanical properties of (Cu-Al-Ni). The Al₂O₃ nanoparticle was added in (3,5,8) wt% to the alloy, the samples were manufactured using powder metallurgy. X-ray diffraction (XRD) and field emission scanning electron microscope (FESEM) with energy-dispersive X-ray spectroscopy were used to analysis the result. The porosity percentage and micro hardness of the Cu-Ni/Al₂O₃ Nano composites increased with the increasing concentration of Al₂O₃, while the density decreased and SME% decreased.

(Myasar, 2023) The impact of incorporating a specific percentage of Aluminum nanoparticles into the Cu-Al-Ni alloy on its mechanical and physical characteristics. The samples were manufactured by powder metallurgy. Physical inspections were performed (using X-ray diffraction and electron microscopy). Mechanical tests included (shape memory effect). The outcomes demonstrated that the inclusion of nanoparticles enhanced the rate of full recovery and partial recovery.

In previous research, the effect of adding other additives on mechanical properties was studied. And other researchers used the Taguchi technique. The aim of the present study it will be study the effect of adding copper nanoparticles on shape recovery and analyzing the results by using the Taguchi technique.

2. MATERIALS AND METHODS

2.1 Design of Experiments (Taguchi Orthogonal Array)

In this experiment, two process parameters (nano copper and copper) will influence the recovery property of a smart alloy. Every parameter was selected at three levels based on the weight ratio of adding nanocopper. The process parameters are selected using a suitable orthogonal array. The Taguchi technique uses orthogonal arrays (OA), a special kind of array; these orthogonal arrays provide all the necessary information about the two process parameters that are selected and affect the process performance. They are used for experimentation. In this experimental work, it has considered three levels and the corresponding factors have resulted in the (L9) orthogonal array as shown in **Table 1**.

Table 1. Process parameters and levels

Parameters	Levels		
	Level 1 at 0% nano	Level 2 at 3% nano	Level 3 at 5% nano
Nano copper (g)	0	0.25	0.415
Copper (g)	8.3	8.05	7.885

In this work, as shown in **Table 2**, Taguchi's method (**Raghu et al., 1991**) is used to design an orthogonal array of (L9) creating nine test conditions with a software application



(Minitab, 2023). Nine experiments must be carried out, produced, and examined, and the data entered into the orthogonal array.

Table 2. L9 Orthogonal array for experimental layout

Factor A (nano)	Factor B (Cu)	Exp.	Factor A (nano) (g)	Factor B (Cu)(g)
1	1	Sc1	0	8.3
1	2	Sc2	0	8.05
1	3	Sc3	0	7.885
2	1	Sc4	0.25	8.3
2	2	Sc5	0.25	8.05
2	3	Sc6	0.25	7.885
3	1	Sc7	0.415	8.3
3	2	Sc8	0.415	8.05
3	3	Sc9	0.415	7.885

2.2 Experimental Works

In this research, the alloy used consisted of (83% Copper, 13% Aluminum, and 4% Nickel powders) adding to them copper nano after preparing the powders and nano copper and then testing them using scanning electron microscopy (SEM) and energy-dispersive X-ray to make sure of the shape of particles and the purity of metal **Table 3.** shows the powders used in the research.

Table 3. Powder used in preparing alloy

No.	Materials	Purity	Particles shape	Particles size	Origin
1	Copper (Cu)	97.6	Spherical	425mesh	USA
2	Aluminum (Al)	96.4	Acicular	250mesh	England
3	Nickel (Ni)	98.8	Spongy	200mesh	China
4	Copper nanoparticles	98.1	Spherical	10-30 nm	China

2.2.1 Methodology

Based on the experiments proposed by the taguchi orthogonal array, nine experiments were conducted. For each experiment, two samples were manufactured, and the average was taken. Thus, the number of samples was eighteen samples were manufactured using the powder metallurgy technique, which consists of three stages (mixing, compacting, and sintering) (Joesph and Ronald, 2008; Mikell, 2010; Serope and Steven, 2010). To achieve the best mixing performance, the powder is first mixed using a horizontal mixing device, which was made by the author. The mixing process was for six hours at a speed of (71) rpm after the percentage weight had been weighed using a sensitive balance. To achieve optimal mixing with 1% acetone of the volume of mixing powder for lubrication and to avoid segregation due to varying densities of the alloying elements, the powder is placed in a glass container at 40% of its volume, as shown in **Fig. 2.**

In the second stage, the samples were compressed in two directions using an electric press machine with punches and a die. The samples are shaped cylindrical and have dimensions of (11) mm in diameter, (16) mm in length, and (10) g in weight. They were pressed at room temperature and (650) MPa of pressure. Twenty minutes was the critical time for pressing the cylindrical sample, and two minutes was the holding time. To lessen friction between the

powder particles and the mold walls, an oiler with a density of 0.88 g/cm^3 was utilized, as shown in **Fig. 3**.

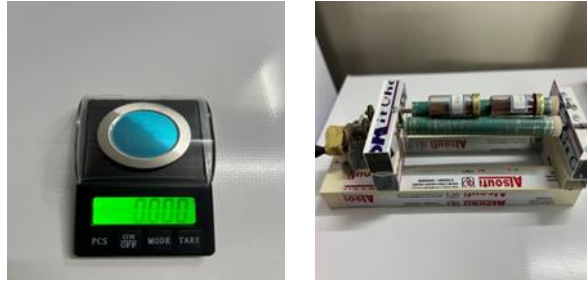


Figure 2. Sensitive balance, Mixing device



Figure 3. Tools used to manufacture the samples, the compression machine, and the samples after compression.

The samples' sintering procedure was carried out in the third step. The objective is to achieve the austenite phase and strengthen the samples. The samples are put inside the combustion chamber's electric furnace. To stop oxidation and remove the gases released during the process that could harm the samples, the furnace is equipped with an insulation system that uses inert gas from argon. There are two stages to the sintering process, as shown in **Fig. 4**. In the first step, the samples were heated to ($500 \text{ }^\circ\text{C}$) for one hour at a rate of ($15^\circ\text{C}/\text{min}$) from room temperature. After that, they were raised to ($850 \text{ }^\circ\text{C}$) for five hours at a rate of ($7 \text{ }^\circ\text{C}/\text{min}$), and the samples were allowed to cool in the furnace (**Zainab and Muradha, 2021**).

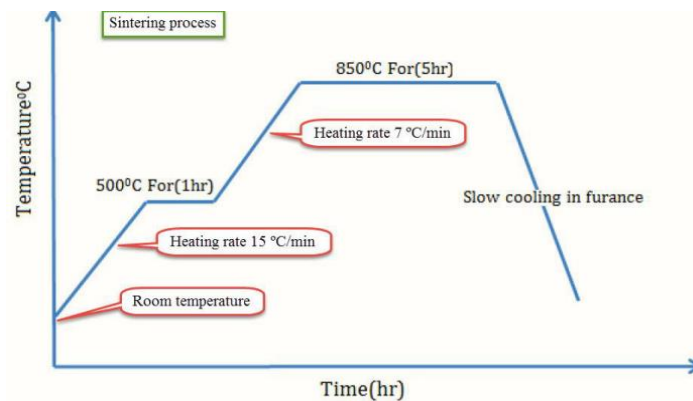


Figure 4. Thermal cycle of the sintering process (**Taher and Ahmed, 2018**)

Heat treatment was applied to the sample after it had finished being manufactured to initiate and stabilize the martensitic phase (**Nawal and Abdul Raheem, 2021**). There were two stages to the heat treatment process. To obtain the martensite phase, the samples were heated in the first stage(a), known as quenching, from room temperature to (800° C) at a rate of (12°) C/min for an hour. After that, the samples were quickly cooled in ice water. To stabilize the martensite phase, the sample was heated in the second stage(b) (ageing) for two hours, from room temperature to (100° C) at a rate of (20°) C/min (**Davis, 2001**), as shown in **Fig. 5**.

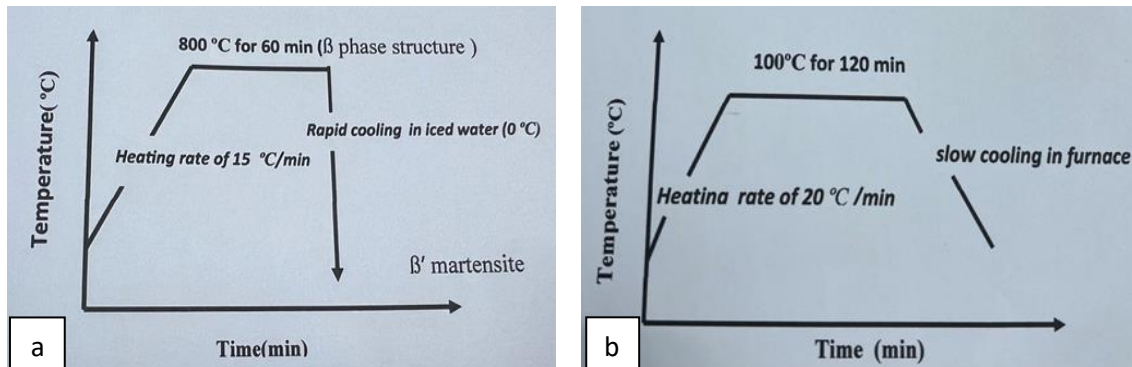


Figure 5. Thermal cycle of heat treatment process (a) quenching (b) ageing (**Sara, 2015**).

2.2.2 Physical and Mechanical Tests

2.2.2.1 Physical Test

The manufactured samples underwent the following physical tests to determine the phase responsible for shape recovery for this type of alloy:

1. Scanning Electron Microscopy (SEM): This test was used to show the layers of martensite after heat treatment.
2. X-ray diffraction (XRD): This test was used to confirm the existence of the martensite phase.

2.2.2.2 Mechanical Test (Recovery Test)

This test was conducted on samples compressed by (1%) of their original length using a computerized uniaxial compression machine. The samples were then heated to (250) °C using a vacuum furnace system, held for five minutes, and allowed to cool in the air. This method allowed for the restoration of the original shape, and the equation was then used to determine the shape memory effect (SME) (**Sara, 2015**).

$$\text{SME} = \frac{L2 - L1}{L0 - L1} * 100\%$$

L0 = the original sample length (mm).

L1 = the sample length after n % compacting process (mm).

L2 = the sample length after heating (mm).

Several times over, increase the compression force in the preceding step until the sample is unable to return to its original length or breaks. The goal of the test is to ascertain how



different ratios of nanoparticles affect the shape memory effect. The results of this test are listed in **Table 4**.

Table 4. Results of shape memory test

Sc1						Sc2					
RS %	L0 mm	L1 mm	L2 mm	SME%	Average	RS%	L0 mm	L1 mm	L2 mm	SME%	Average
1	16.32	16.25	16.32	100	100	1	16.79	16.62	16.79	100	100
	16.22	16.15	16.22	100			16.52	16.45	16.52	100	
2	16.32	16.1	16.32	100	100	2	16.79	16.55	16.79	100	100
	16.22	15.99	16.22	100			16.52	16.28	16.52	100	
3	16.32	15.93	16.32	100	100	3	16.79	16.48	16.78	96.7	96
	16.22	15.82	16.22	100			16.52	16.22	16.50	95.3	
4	16.32	15.68	16.3	96.8	96.9	4	16.78	16.20	16.71	87.9	88.54
	16.22	15.57	16.2	97			16.50	15.94	16.44	89.2	
5	16.3	15.58	16.22	88.8	86.6	5	16.71	15.87	16.55	80.9	79
	16.2	15.43	16.08	84.41			16.44	15.62	16.25	76.8	
6	16.22	15.34	16.13	79.5	78.2	6	16.55	15.65	16.27	68.8	71.1
	16.08	15.21	15.88	77.01			16.25	15.27	15.99	73.4	
7	16.13	15	15.75	66.3	71.3	7	16.27	15.23	15.88	62.5	60
	15.88	14.86	15.64	76.4			15.99	14.98	15.57	58.4	
Sc3						Sc4					
RS %	L0 mm	L1 mm	L2 mm	SME%	Average	RS%	L0 mm	L1 mm	L2 mm	SME%	Average
1	16.35	16.28	16.35	100	100	1	16.11	15.97	16.11	100	100
	16.64	16.57	16.64	100			16.25	16.08	16.25	100	
2	16.35	16.12	16.35	100	100	2	16.11	15.88	16.11	100	100
	16.64	16.40	16.64	100			16.25	16.03	16.25	100	
3	16.35	15.92	16.32	93.02	94.01	3	16.11	15.72	16.08	92.3	91.3
	16.64	16.24	16.62	95			16.25	15.96	16.22	90.4	
4	16.32	15.76	16.23	83.9	83.15	4	16.08	15.43	15.92	75.3	78.5
	16.62	16.05	16.52	82.4			16.22	15.67	16.12	81.8	
5	16.23	15.45	16.06	78.2	73.6	5	15.92	15.12	15.68	70	71.4
	16.52	15.89	16.23	69			16.12	15.31	15.9	72.8	
6	16.06	15.19	15.71	59.7	68.4	6	15.68	14.73	15.33	63.1	66.4
	16.23	15.35	16.03	77.2			15.9	14.94	15.61	69.7	
7	15.71	14.62	15.26	57.7	54.6	7	15.33	14.25	14.8	51.4	52.4
	16.03	15.1	15.58	51.6			15.61	14.51	15.1	53.6	
Sc5						Sc6					
RS %	L0 mm	L1 mm	L2 mm	SME%	Average	RS%	L0 mm	L1 mm	L2 mm	SME%	Average
1	16.93	16.82	16.93	100	100	1	16.9	16.82	16.9	100	100
	16.85	16.71	16.85	100			16.81	16.71	16.81	100	
2	16.93	16.74	16.93	100	100	2	16.9	16.67	16.9	100	100
	16.85	16.61	16.85	100			16.81	16.56	16.81	100	
3	16.93	16.62	16.9	90.3	88.6	3	16.9	16.59	16.85	83.8	85.4
	16.85	16.54	16.81	87.1			16.81	16.40	16.76	87	
4	16.9	16.22	16.73	75	74	4	16.85	16.27	16.66	67.2	68.9
	16.81	16.13	16.62	72.05			16.76	16.18	16.59	70.6	
5	16.73	15.89	16.45	66.6	68.6	5	16.66	15.82	16.34	61.9	63.4
	16.62	15.7	16.35	70.6			16.59	15.76	16.3	65	
6	16.45	15.45	16.06	61	63.3	6	16.34	15.35	15.94	60.4	58.2

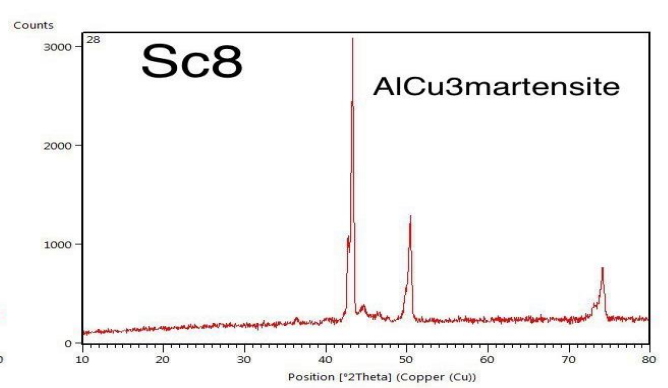
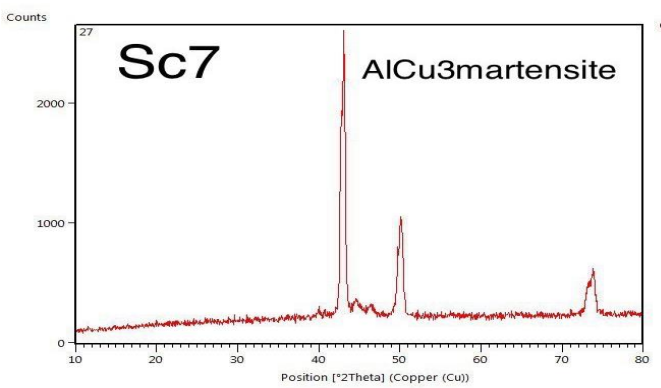
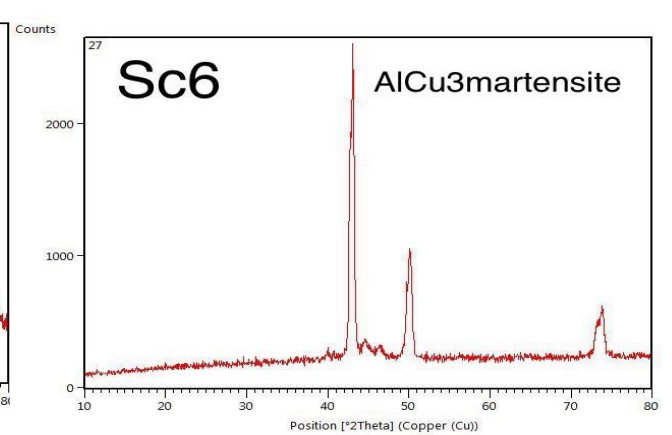
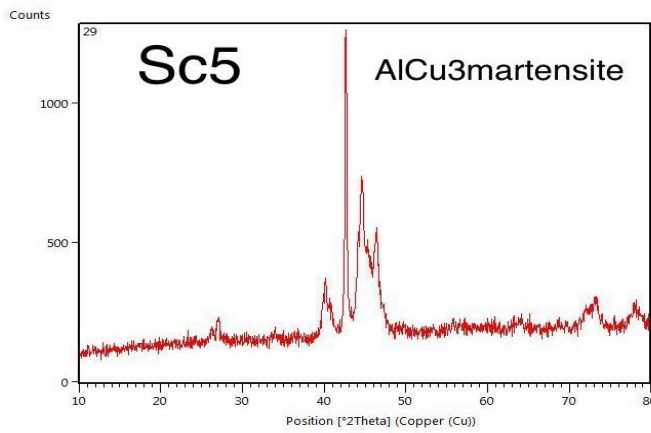
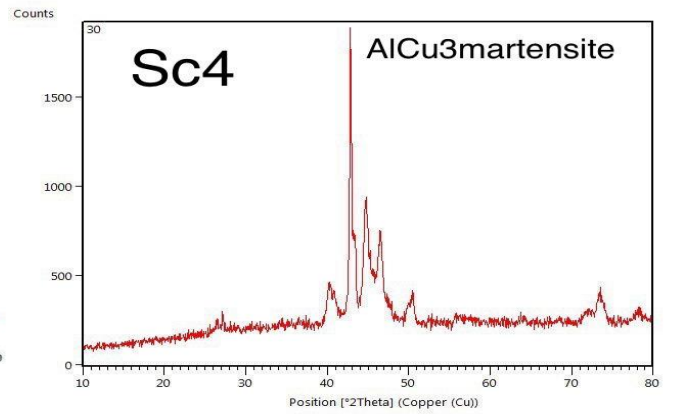
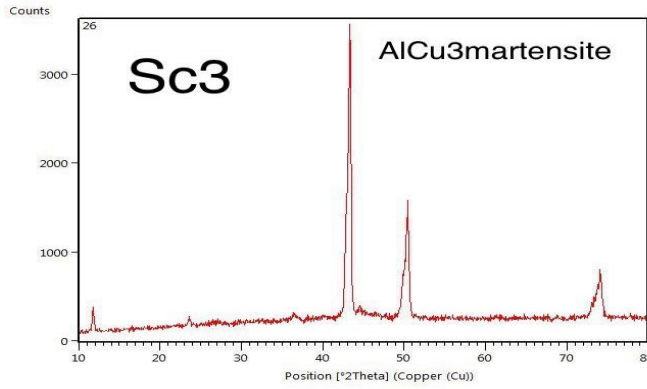
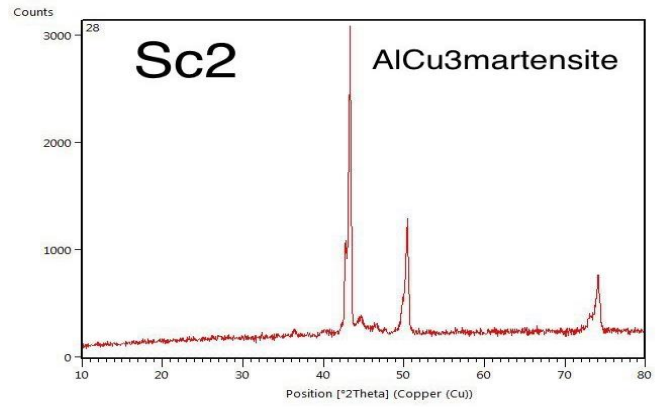
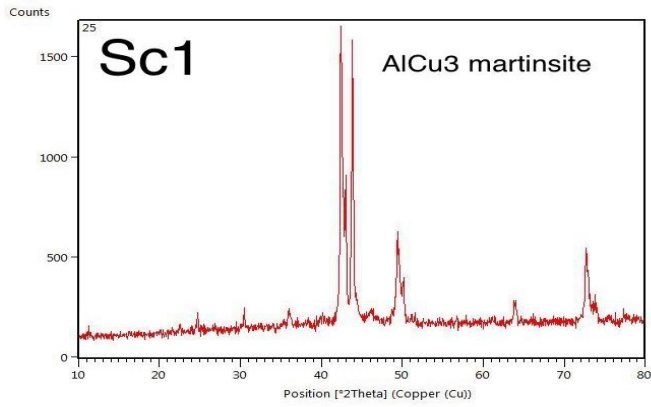


	16.35	15.36	16	65.6			16.3	15.32	15.87	56.1	
7	16.06	14.93	15.53	53	50.15	7	15.94	14.82	15.3	42.8	46.4
	16	14.88	15.41	47.3			15.87	14.75	15.31	50	
Sc7						Sc8					
RS %	L0 mm	L1 mm	L2 mm	SME%	Average	RS%	L0 mm	L1 mm	L2 mm	SME%	Average
1	16.74	16.62	16.74	100	100	1	16.78	16.61	16.78	100	100
	16.69	16.50	16.69	100			16.74	16.59	16.74	100	
2	16.74	16.50	16.74	100	100	2	16.78	16.54	16.78	100	100
	16.69	16.39	16.69	100			16.74	16.43	16.74	100	
3	16.74	16.33	16.68	85.3	82.9	3	16.78	16.37	16.7	78	81.9
	16.69	16.28	16.61	80.4			16.74	16.33	16.68	85.8	
4	16.68	16.01	16.45	65.6	64.8	4	16.7	16.03	16.45	62.6	58.9
	16.61	15.94	16.37	64.1			16.68	16.01	16.38	55.2	
5	16.45	15.62	16.11	59	59.9	5	16.45	15.62	16.07	54.2	55.7
	16.37	15.55	16.05	60.9			16.38	15.56	16.03	57.3	
6	16.11	15.14	15.64	51.5	53	6	16.07	15.1	15.5	46.3	47.8
	16.05	15.08	15.61	54.6			16.03	15.06	15.54	49.4	
7	15.64	14.54	15.04	45.4	44.5	7	15.5	14.41	14.8	41.2	40.75
	15.61	14.51	14.9	43.6			15.54	14.45	14.9	40.3	

Sc9					
RS %	L0 mm	L1 mm	L2 mm	SME %	Average
1	16.35	16.21	16.35	100	100
	16.84	16.69	16.84	100	
2	16.35	16.02	16.35	100	100
	16.84	16.60	16.84	100	
3	16.35	15.95	16.28	82.5	79.6
	16.84	16.43	16.74	75.6	
4	16.28	15.72	16.05	58.9	55.9
	16.74	16.1	16.46	53	
5	16.05	15.2	15.6	47	44
	16.46	15.63	15.97	41	
6	15.6	14.66	15	43.6	40
	15.97	15	15.41	41.7	
7	15	13.95	14.36	39.1	38.15
	15.41	14.33	14.73	37.21	

3. RESULTS AND DISCUSSIONS

1. The data analysis indicates the presence of the martensitic phase (AlCu₃) in the samples after comparing the XRD test results with standard peaks and test equipment tables. All of the study samples developed the martensitic phase, which is the primary factor causing shape recovery; this suggests that the sintering, quenching, and aging processes were successful because they produced the martensite phase in every sample used in this experimental work. The analysis results show that all the samples have the same crystalline microstructure of the martensitic phase. Considering that every sample appears in the martensite phase (AlCu₃), as shown in Fig. 6



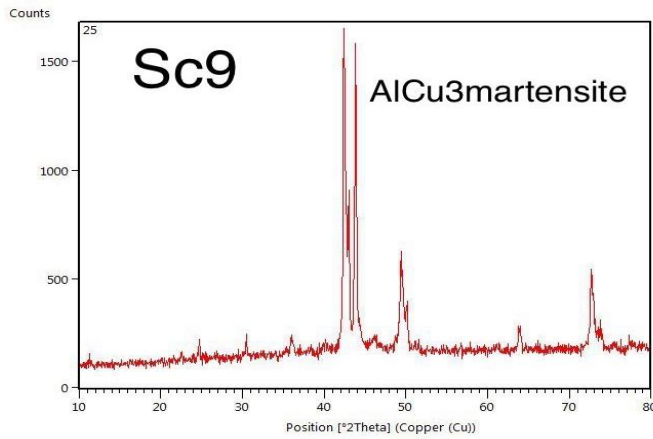


Figure 6. Results of XRD test for manufacturing samples

2. The findings of a test using scanning electron microscopy which was done to examine the sample's structure following heat treatment (quenching and aging) and to determine its martensite phase. An increase in the martensite layer has been observed, and they are more pronounced in samples with a higher percentage of copper nano (Sc9) when compared with samples with zero nano (Sc1). Likewise, for the (Sc2) sample, if compared to the sample (Sc1), it has been noticed an increase in martensite layers, as well as for the rest of the samples. It can be said that increasing the percentage of nano addition leads to an increase in the martensite layer, as shown in **Fig. 7**

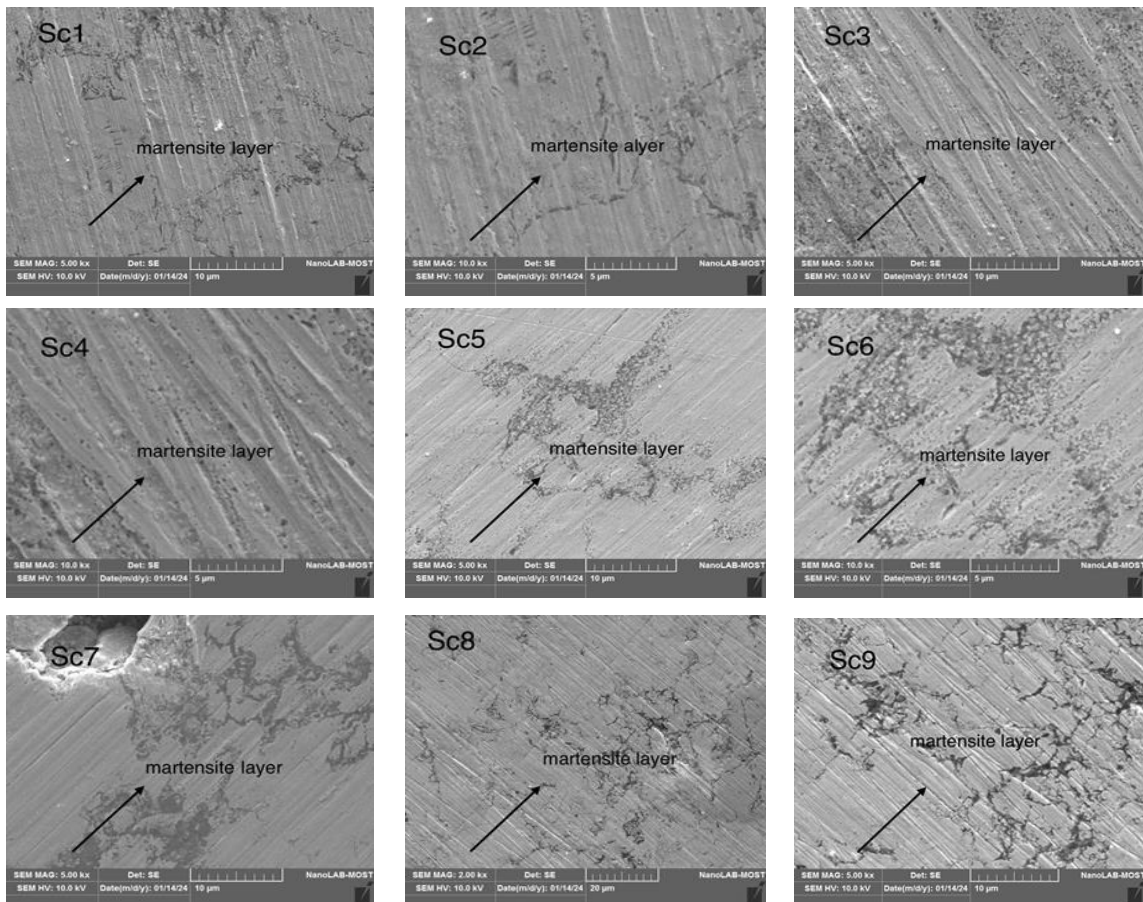


Figure 7. Results of SEM images for manufacturing sample.



3. Table 4. Show the results of the shape memory effect test. It was noted for the same conditions, all samples in this test behaved uniformly at a compression ratio of 2% of the original length of the specimens under study, where the recovery was 100% complete. The behavior of the specimen changed when the compression ratio was set at 3% of the initial length. It was noted sample (Sc1) succeeded in recovering 100% while (Sc2) recovered (96%), sample (Sc3) recovered (94.1%), sample (Sc4) recovered (91.3%), and so on for the rest of the sample. It can be said the addition of nano copper to this alloy did not improve recovery properties, when the percentage of copper nano addition increased, the recovery strain became low. This was also observed regarding the increase in compression at (4%), (5%), and so on until the sample failed to return to its original shape. The reason behind the recovery decline is the homogeneity in the nanoparticle distribution among the alloy's constituent grains; as a result, there is less porosity between the particles, which raises the hardness, when the hardness increases, the recovery declines because they are in an inverse relationship.

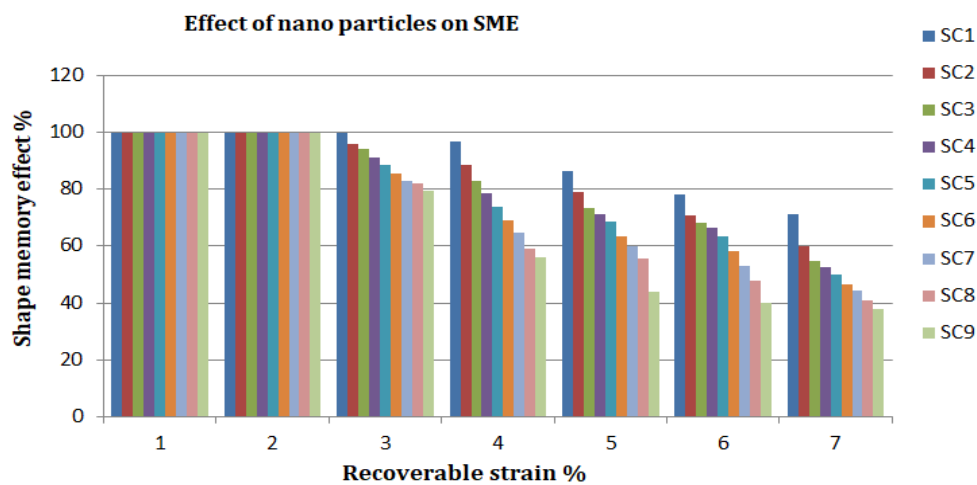


Figure 8. The effect of nanoparticle ratios on recoverable strain and shape memory effect

Fig. 8 shows the effect of copper nano on the shape memory effect for samples (Sc1 to Sc9). It was found that the sample Sc1 with zero nano addition gave the best value of SME%, while the sample Sc9 with a high percentage of nano gave the lowest value of SME%.

4. After getting the results of the shape memory effect test, it will be applied to the Taguchi orthogonal array and filled with results. In this research, we will choose the recovery results at a compression ratio of 4% and perform the analysis of the signal to Noise ratio (S/N) and ANOVA analysis. **Table 5.** shows taguchi orthogonal array filling with recovery results. The shape effect becomes the response in the Taguchi orthogonal. The results have been analyzed by using the (S/N) ratio to give the optimal level for each process parameter that corresponded to the large (S/N) ratio and ensure the highest value of the shape memory effect. The main effect of each parameter at three different levels on the mean and (S/N) ratio for (SME) are shown in **Table 6.** Based on the large (S/N) ratio, the optimum condition at (nano (A) = 0, and Cu (B) = 8.3) from the main effect of the S/N ratio. The effect of each parameter is calculated by the difference (delta) between the higher and lower values of the level for each factor. The most significant factor that affected the shape memory effect is nano copper followed by copper as indicated in Rank.



Table 5. Taguchi orthogonal array filling with results

Exp.	Factor A (nano)	Factor B (Cu)	SME%
SC1	0	8.3	96.9
SC2	0	8.05	88.54
SC3	0	7.885	83.15
SC4	0.25	8.3	78.5
SC5	0.25	8.05	74
SC6	0.25	7.885	68.9
SC7	0.415	8.3	64.8
SC8	0.415	8.05	58.9
SC9	0.415	7.885	55.9

Signal To Noise ratio (S/N)

Table 6. The main effect and (S/N) ratio

Mean for SME			(S/N) ratio for SME		
Levels	A (nano)	B Cu)	Levels	A (nano)	B (Cu)
1	89.53	80.07	1	39.02	37.95
2	73.80	73.81	2	37.35	37.24
3	59.87	69.32	3	35.53	36.90
Delta	29.66	10.75	Delta	3.49	1.25
Rank	1	2	Rank	1	2

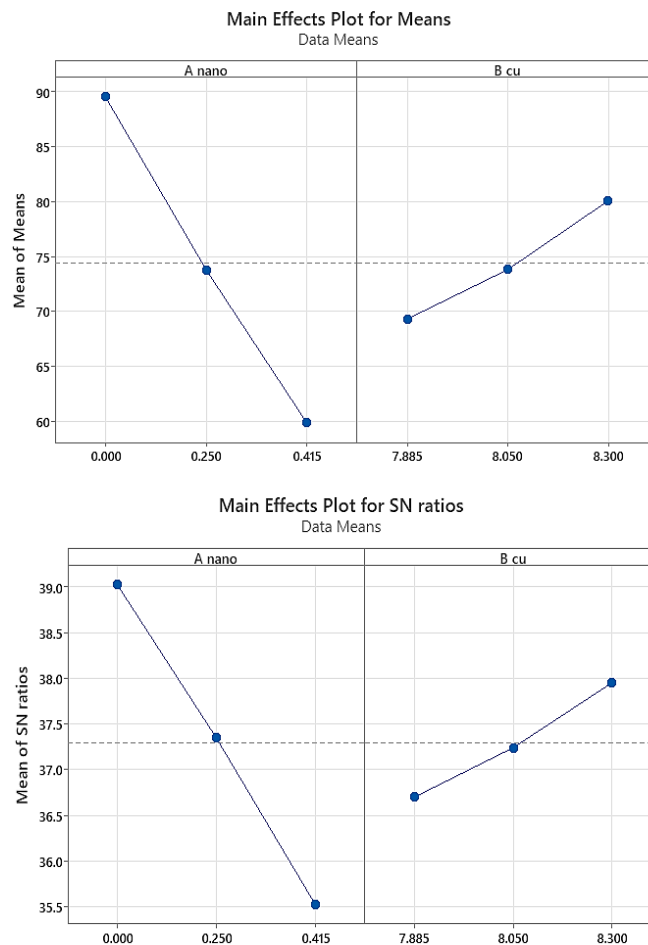


Figure 9. The main effect plot of mean and (S/N) ratio for the shape memory effect.



The Analysis of Variance (ANOVA) Technique is conducted on shape effect % to investigate the contribution of parameters on the response as shown in **Table 7**.

Table 7. ANOVA analysis for SME%

Source	DOF	SST	MS	P contribution %
A	2	1321.48	660.742	87.82
B	2	174.89	87.443	11.62
Error	4	8.26	2.065	
Total	8	1504.63		

Table 7. shows the ANOVA analysis for (SME %). The contribution of the parameter (nano) is (87.82 %) and the contribution of the parameter (cu) is (11.62%), so it is clear that nano copper is the most contributing factor (SME%).

4. CONCLUSIONS

The raw material particles interact more effectively because of their different shapes and sizes, increasing their bonding force and reducing porosity and voids. Physical tests show that an increase in the martensite layer (Al₃cu) corresponds to an increase in the percentage of copper nanoparticles. This phase, which is thought to have a higher hardness than other structural phases, consequently reduces porosity. Using the Taguchi method, the number of experiments needed was reduced by employing a suitable orthogonal array, making it more cost-effective and time compared to the traditional method. In the recovery to the original length test. The best recovery was at a ratio (0%) with the nano-addition of copper. The higher the percentage of nano leads to a reduction in shape recovery, as this was observed in the sample with (0.415 %) nano addition. The addition of nanoparticles did not produce better recovery results than without addition. Based on the (S/N) ratio results for shape recovery for the given set of parameters, the optimum conditions were found at the zero nano copper ratio and (8.3%) copper. The most significant factor that affected shape recovery was nano-copper, followed by copper. From ANOVA analysis of results for shape recovery, the most contribution parameter was copper nano at a percentage (87.82%) followed by copper with a contribution percentage (11.62%).

NOMENCLATURE

Symbol	Description	Symbol	Description
SMAs	Shape memory alloys.	XRD	X-ray diffraction
A	Austenite phase.	MESH	Count the number of openings in one linear inch of screen.
M	Martensite phase.	R.P.M	Revolutions per minute .
SME	Shape memory effect.	S/N	Signal to Noise ratio
MF	Martensite finish temperature.	ANOVA	Analysis of Variance
AF	Austenite finish temperature	OA	Orthogonal array.
PM	Powder metallurgy	DOF	Degree of freedom
SEM	Scanning electron microscope	SST	Total sum of square
EDX	Energy dispersive x-ray	MS	Mean square



Acknowledgments

Special thanks to the members of the engineering workshop of the Department of Mechanical Engineering, University of Baghdad, especially to Mr. Khalil Ahmed Wadi, for providing assistance in completing this work.

Credit Authorship Contribution Statement

Dilsuz. A: Writing – review & editing, Writing – original draft, Validation, Software, Methodology, data collection. Ahmed Al Kafaji: review & editing, Validation.

Declaration of Competing Interest

The authors declare that they have no known competing financial interests or personal relationships that could have appeared to influence the work reported in this paper.

REFERENCES

- Ahmed, A., 2018. Effect of Cu-Al proportions in smart (Cu-Al-Ni) alloy for best mechanical properties by using artificial intelligence. *International Journal of Mechanical Engineering and Technology*, 25(1), pp.11-22.
- Ahmed, A., Sara, J., 2016. Effect of compaction pressure and sintering temperature on shape effect and compression strength of Cu-Al-Ni shape memory alloy. *Journal of Association of Arab Universities for Engineering Studies and Research*, 2(23).
- Al-Humairi, S.N.S., 2020. Cu-based shape memory alloys: Modified structures and their related properties. *Recent Advancements in Metallurgical Engineering and Electrodeposition*. <https://doi.10.5772/intechopen.86193>.
- Amir, A., N. Anuradha., 2018. Use of orthogonal arrays and design of experiment via Taguchi L9 method in probability of default. *Accounting*, (4), pp.113–122. <https://doi.10.5267/j.ac.2017.11.001>.
- Christian, L., 2013. Some general points about SMA in Shape Memory Alloy Handbook. Britain and the USA: ISTE Ltd and John Wiley & Sons. ISBN:978-1-848-21434.
- Corneliu, C., 2010. Shape memory alloy. Portugal: Jeeza Trdine. ISBN: 978-953-307-106-0.
- Davis, JR. 2001. Copper and Copper alloy. USA: ASM international. ISBN: 978-0-87170-726-0.
- Gabriele, B., Giorgia, F., Salvatore A., Andrea, S. 2023. Performance of smart materials-based instrumentation for force measurements in biomedical applications a methodological review. *Actuators*, 12(261). <https://doi.org/10.3390/act12070261>
- Hasan., 2016. *Prediction of Mechanical Properties of Smart Alloy Cu-Al-Ni based on Sintering Time by Using ANN*. M.Sc. thesis, College of Engineering, University of Baghdad, Baghdad, Iraq.
- Joseph T. Black, Ronald A., 2008. Materials & processes in manufacturing. USA: John Wiley & Sons, INC. ISBN:11189876775.
- Kumar L., 2017. Optimization of MiG welding process parameters for improving welding strength of steel. *International Journal of Engineering Trends & Technology*, 50 (1), pp.26-33. <https://doi.10.14445/22315381/IJETT-V50P205>.



Lagoudas, DC., 2008. Shape Memory Alloys: Modeling and Engineering Applications. United States: Springer. ISBN: 978-0-387-47684-1.

Manianb, B., 2021. Application of shape memory alloys in engineering – A review. *Journal of Physics Conference Series*, 2054(1) <https://doi.org/10.1088/1742-6596/2054/1/012078>.

Mikell, M., 2010. Fundamentals of modern manufacturing materials, processes, and systems. USA: John Wiley & Sons, INC. ISBN: 978-1-119-47521-7.

Mohammed, S.H. and Shahatha, S.H., 2023, May. Shape memory alloys, properties and applications: a review. In *AIP Conference Proceedings* (Vol. 2593, No. 1). AIP Publishing.

Morales, L., Fady, A., Stefan, Z., Miguel, B., Shao-Pu, T., Jer-Ren, Y., Dierk, R., Carlos, G., Francisca, C., 2018. Crystallographic examination of the interaction between texture evolution, mechanically induced martensitic transformation, and twinning in nanostructured bainite. *Journal of Alloys and Compounds*, 752, p.p. 505-519. <https://doi.org/10.1016/j.jallcom.2018.04.189>

Myasar, A., Ahmed, A., 2023. Study the effect of adding Aluminum nanoparticles to a smart alloy (Cu-Al-Ni) on hardness and porosity. *Journal of Engineering*, 29(2), pp.1-15. <https://doi.org/10.31026/j.eng.2023.02.01>

Nashwan, Q., Yad, T., Mohammed, H., Mohammed, A., Peter, B., 2024. Experimental investigation of the surface roughness for Aluminum Alloy AA6061 in milling operation by Taguchi method with the ANOVA technique. *Journal of Engineering*, 30(3), pp.1-14. <https://doi.org/10.31026/j.eng.2024.03.01>

Nawal, M., Abdul Raheem, K., 2021. Influence of Titanium additions on the corrosion behavior of Cu-Al-Ni shape memory alloy. *Materials Science Forum*, (1021), pp. 55-67. <https://doi.org/10.4028/www.scientific.net/MSF.1021.55>

Omkar M., Kaulgud1., Sandip T. 2022. Process parameter optimization of TIG welding by Taguchi method and its effect on performance parameter of stainless steel grade 302HQ. *International Transaction Journal of Engineering, Management, & Applied Sciences & Technologies*, 13 (7), pp.1-10. <https://doi.org/10.14456/ITJEMAST.2022.132>.

Othmane, B., 2020. Shape memory alloy, high Temperature, and Smart Alloys Branch. USA: NASA Glenn Research Center. ISBN: 978-0-387-47685-8.

Otsuka, K., Wayman, CM., 1999. Shape Memory Materials. Reprint. Illustrated ed. London, UK: Cambridge University Press. ISBN 0521 44487 X hardback.

Praveen, N., Mallik, U.S., Shivasiddaramaiah, A.G., Hosalli, R., Prasad, C.D. and Bavan, S., 2024. Machinability study of Cu-Al-Mn shape memory alloys using Taguchi method. *Journal of The Institution of Engineers (India): Series D*, pp.1-13. <https://doi.org/10.1007/s40033-023-00629-w>

Raghu, N., Erics, S., Lagergren, James J., 1991. Taguchi orthogonal arrays are classical design of experiments. *NLST Journal of research*, 96(5), pp. 577-591. <http://doi.org/10.6028/jres.096.034>.

Raed, N., Khalid, H., Ahmed, T., Abdulhameed, M., Saif, I., 2018. The physical and mechanical properties of a shape memory alloy reinforced with carbon nanotube (CNTs). *Tikret Journal for Pure Science*, 23(9), pp.80-88. <https://doi.org/10.25130/tjps.v23i9.816>



- Raed, N., Omer, J., 2020. Influences of Mg Addition on the mechanical properties of Cu- Al- Ni shape memory alloy. *Tikrit Journal for Pure Science*, 27(3), pp.82-93. <http://doi.org/10.25130/tjes.27.3.10>
- Sadashiva M, M., Yunus, S., Nouman, K. Ramesh, K., T.M.Deve, G., 2021. A review on application of shape memory alloys. *International Journal of Recent Technology and Engineering*, 9(6). <https://doi.10.35940/ijrte.F5438.039621>.
- Safi, S., Moneer, T., Muhsin, J., 2024. Optimization and simulation parameters of the resistance spot welding for commercial aluminium (AA1050) at low power welding machine. *Journal of Engineering*, 30(4), pp. 57-71. <https://doi.org/10.31026/j.eng.2024.04.04>
- Sara J., 2005. *Process Parameters Optimization of Shape Memory (Cu-Al-Ni) Alloy Using Taguchi Technique*. M.Sc. thesis, College of Engineering, University of Baghdad, Baghdad, Iraq.
- Serope, K., Steven, R., 2010. Manufacturing engineering and technology. New Jersey: Pearson Education, INC. ISBN-13: 978-0-13-522860-9.
- Safa, N., Hamzah, E., Abubaker, T., Bakhsheshi, H., Saeed, F., 2014. Influence of silver nanoparticles addition on phase transformation, mechanical properties and corrosion behavior of Cu- Al-Ni shape memory alloys. *Journal of alloys and compounds*, 612, pp.471-478. <http://dx.doi.org/10.1016/j.jallcom.2014.05.173>
- Samudrapom, D., 2022. Altering nanoparticle content to improve Copper-based composites. *Nano Technology Journals*, <https://www.azonano.com/news.aspx?newsID=38645>
- Taher, M., and Ahmed A., 2018. *Study the Mechanical Properties of Ternary (Cu-Al-Ni) Shape Memory Alloys Affected by (Al-Ni) and (Cu-Ni) Contents Enhancement with ANN*. M.Sc. thesis, College of Engineering, University of Baghdad, Baghdad, Iraq.
- Takale, A. and Chougule N., 2019. Optimization of process parameter of wire electro discharge machining for Ti_{49.4} Ni_{50.6} shape memory alloy using Taguchi technique. *International Journal of Structure Integrity*, 10(4), pp. 548-568. <https://dx.doi.org/10.2139/ssrn.3101586>
- Malinin, V.G., Malinina, N.A., Malinin, G.V. and Malukhina, O.A., 2018, October. Development of methods of structural-analytical mesomechanics that take into account the statistical properties of martensitic transformations in materials with shape memory effect. In *IOP Conference Series: Materials Science and Engineering* (Vol. 441, No. 1, p. 012030). IOP Publishing. <https://doi.10.1088/1757-899X/441/1/012030>.
- Zainab, S., Murtadha, A., 2021. Effect of Ag nanoparticles addition on the microstructure of Cu-21%Zn-6%Al shape memory alloys. *Basra Journal for Engineering Science*, 21(3), pp.42-49. <http://dx.doi.org/10.33971/bjes.21.3.5>



استخدام تقنية تاكوشي لدراسة تأثير إضافة نانو نحاس على تأثير ذاكرة الشكل لسبيكة ذكية (Cu- Al- Ni)

دلسوز عبد الستار عبد الجبار*، احمد عبد الرسول احمد الخفاجي

قسم الهندسة الميكانيكية، كلية الهندسة، جامعة بغداد، بغداد، العراق

الخلاصة

يهدف هذا البحث إلى تقليل عدد التجارب باستخدام تقنية تاكوشي وسيتم تطبيقها على إضافة جزيئات النحاس النانوية ودراسة تأثيرها على استعادة الشكل لسبيكة ذات ذاكرة شكلية (Cu-13% Al- 4%Ni %83). وتم إضافة نسب مختلفة من النانو إلى السبيكة مقابل تغيير نسبة النحاس مع الحفاظ على ثبات نسب النيكل والألمنيوم. استخدمت تقنية تعدين المساحيق صناعة العينات. تم إجراء نوعين من الاختبارات: الاختبارات الفيزيائية، بما في ذلك حيود الأشعة السينية (XRD) والمجهر الإلكتروني الماسح (SEM)، تم استخدامها لفحص المواد الخام قبل التصنيع وفحص العينات بعد التصنيع. تم إجراء اختبار ميكانيكي لتأثير ذاكرة الشكل (SME%) لنسبة ضغوط مختلفة. تشير النتائج إلى أن إضافة النحاس النانوي قلل من استعادة الشكل عند نسبة ضغط (3%). أظهر تحليل النتائج الممثلة بنسبة الإشارة إلى الضوضاء (S/N) وتحليل التباين (ANOVA) أن العامل الأكثر أهمية في استعادة الشكل هو النحاس النانوي يليه النحاس وكان العامل الأكثر مساهمة هو النحاس النانوي بنسبة 87.82%.

الكلمات المفتاحية: تحليل التباين، تقنية تعدين المساحيق، تقنية تاكوشي، نانو نحاس، سبائك الذكية، سبائك متذكّرة الشكل.